Biophysical Chemistry 200–201 (2015) 18–26

Contents lists available at ScienceDirect

Biophysical Chemistry

journal homepage: http://www.elsevier.com/locate/biophyschem

Cyanohydrin reactions enhance glycolytic oscillations in yeast

Bjørn Olav Hald [a,*], Astrid Gram Nielsen [b], Christian Tortzen [b], Preben Graae Sørensen [b]

[a] Department of Biomedical Sciences, University of Copenhagen, Copenhagen, Denmark
[b] Department of Chemistry, University of Copenhagen, Copenhagen, Denmark

HIGHLIGHTS

- Fermenting yeast produce intracellular cyanohydrins if fed with cyanide.
- Yet, extracellular lactonitrile production accounts for ~66% of cyanide consumption.
- During fermentation, cyanide mainly reacts with intracellular carbonyl compounds.
- Intracellular cyanide reactions augment the amplitude of oscillations.

GRAPHICAL ABSTRACT

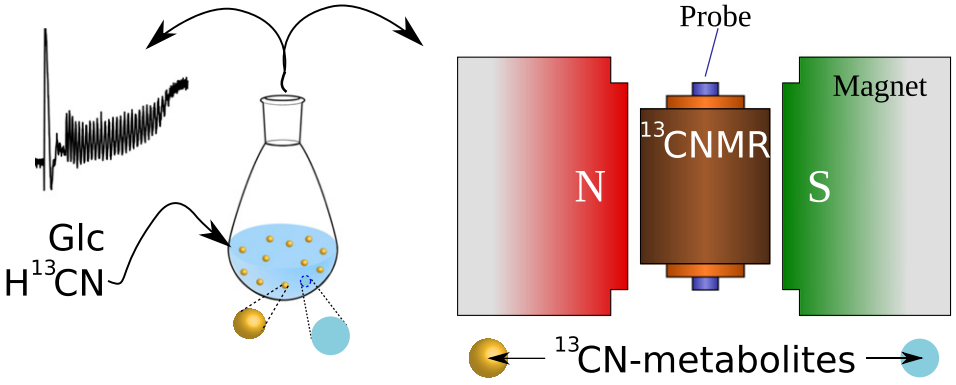

ARTICLE INFO

Article history:
Received 10 February 2015
Received in revised form 16 March 2015
Accepted 17 March 2015
Available online 27 March 2015

Keywords:
Yeast
Oscillations
NMR
Modeling

ABSTRACT

Synchronous metabolic oscillations can be induced in yeast by addition of glucose and removal of extracellular acetaldehyde (ACA_x). Compared to other means of ACA_x removal, cyanide robustly induces oscillations, indicating additional cyanide reactions besides ACA to lactonitrile conversion. Here, ^{13}C NMR is used to confirm our previous hypothesis, that cyanide directly affects glycolytic fluxes through reaction with carbonyl-containing compounds. Intracellularly, at least 3 cyanohydrins were identified. Extracellularly, all signals could be identified and lactonitrile was found to account for ~66% of total cyanide removal. Simulations of our updated computational model show that intracellular cyanide reactions increase the amplitude of oscillations and that cyanide addition lowers [ACA] instantaneously. We conclude that cyanide provides the following means of inducing global oscillations: a) by reducing [ACA_x] relative to oscillation amplitude, b) by targeting multiple intracellular carbonyl compounds during fermentation, and c) by acting as a phase resetting stimulus.

1. Introduction

In a stirred suspension of yeast cells harvested at the diauxic shift, synchronous metabolic oscillations can be induced by addition of glucose and addition of cyanide [1,2]. The mechanism of yeast cell communication and synchronization is still an unresolved question. Extracellular acetaldehyde (ACA_x) seems to be the (main) synchronizing agent [3–5] and hence the synchronization signal depends on the ratio between the oscillatory amplitude and average concentration of ACA_x. However, direct dynamic evidence for [ACA_x]-oscillations in the extracellular medium remains elusive. Removal of ACA_x using e.g. $N_{2(g)}$ has been shown to induce oscillations [6,7]. However, a much stronger propensity to induce oscillations is observed using cyanide [6]. Recently, we found that much cyanide is consumed during fermentation, hypothesizing that cyanide not only reacts with ACA_x, but also

* Corresponding author.
E-mail address: bohald@sund.ku.dk (B.O. Hald).

http://dx.doi.org/10.1016/j.bpc.2015.03.004
0301-4622/

with unidentified intracellular carbonyl compounds [8]. It is well-known that glucose (Glc), fructose (Fru), pyruvate (Pyr), dihydroxyacetone-phosphate (DHAP), and ACA are the major carbonyl compounds produced during fermentation [9]. Using ^{13}C-NMR, we show that Pyr, DHAP, ACA, and smaller sugars readily react with cyanide, while the hexoses only show weak to no reaction in the same reaction conditions used under fermentation. The obtained chemical shifts of these cyanohydrins are used to analyze fermentation of glucose and cyanide. Extracellularly, a single cyanohydrin signal from lacto (lactonitrile) is dominant. The well-defined signal allowed for a quantitative estimate of [lacto] during fermentation. Intracellularly, the presence of at least three intracellular cyanohydrins, most likely from Pyr and intermediary sugars, was confirmed. The data obtained was used to update a computational model which subsequently was analyzed with respect to the ability of cyanide to induce oscillations. Collectively, we show that cyanide predominantly reacts with ACA_x, but also with intracellular carbonyl compounds produced during fermentation. Both modes of reaction increase the amplitude of oscillations. Finally, addition of cyanide may act as a synchronization stimulus, facilitating global oscillations. Why most cyanide reacts with ACA_x, remains however an open question.

2. Materials and methods

2.1. Cell preparation

Yeast cells (*Saccharomyces cerevisiae* X2180) were grown aerobically at 30 °C in a rotary shaker (closed batch culture) to the point of Glc depletion [10]. Harvested cells were washed twice in a 0.1 M potassium phosphate buffer (PBS), pH 6.8, followed by resuspension to the desired cell density. Cell density was determined by optical density (OD), and OD = 20 corresponding to a dry weight of 12.8 mg/ml was chosen. Finally, the cells were starved at 30 °C for 2 h and kept at ~0 °C until start of experiments.

2.2. "Close to fermentation conditions"

All experiments were carried out in conditions that resembled the fermentation conditions as closely as possible. Thus, in all experiments we used 0.1 M PBS at 25 °C and pH 7.2. Unless otherwise indicated, we only used concentrations of cyanide and metabolites that resembled the values found during fermentation (i.e. [HCN] = 5 mM and [metabolite] = 20–30 mM).

2.3. UV-Spectrometry

All spectra were measured using a Perkin-Elmer Lambda 1050 spectrometer fitted with a thermostat (25 °C) and magnetic stirring. Optical spectrometry was performed on pure substances dissolved in 0.1 M PBS and spectra from 200–800 nm were obtained from each substance. Maximal absorbance of ACA and Pyr were found at 278 nm and 320 nm, respectively. HCN did not absorb in these regions. The relative absorptivities were found to be $(0.0075 \pm 0.0006)\ \mathrm{mM^{-1}cm^{-1}}$ for ACA and $(0.0202 \pm 0.001)\ \mathrm{mM^{-1}cm^{-1}}$ for Pyr. In 0.1 M PBS these absorbances were not significantly sensitive to small reaction mediated changes in pH. Cyanohydrins derived from ACA and Pyr showed only little absorbance, but were taken into account. From the kinetic measures of HCN + Pyr ⇌ PyrCN and HCN + ACA ⇌ lacto, the rate constants were determined.

2.4. ^{13}C-NMR

All NMR spectra were measured on a 500 MHz (with a ^{13}C-cryoprobe) instrument. A sealed capillary tube containing DMSO-*d*6 was used in each NMR-tube as the reference for all chemical shift values and as a lock. Field shimming was performed before recording. During fermentation, spectra were obtained using a regular ^{1}H-decoupled pulse with a delay between scans of 2 s and 64 scans per spectra (NS = 64). This setting yielded the shortest acquisition time with consistent areas of signals and provided 9 spectra per fermentation. In experiments where the yeast cell suspension did not ferment glucose, signal-to-noise ratio was improved by increasing NS as indicated. Before these recordings, the extracellular medium was separated from the packed cells by centrifugation (18,000*g*) and cells were washed twice in 0.1 M PBS.

2.5. Analyzing spectra

Free induction decays (FIDs) were analyzed in MestReNova, version 8.1.0 (Mestrelab research S.L. 2012, Santiago de Compostela, Spain). Baseline artifacts produced by the cryoprobe were resolved and spectra were manually phase corrected.

2.6. Internal standard

MeOH was selected as 1) it gives a single signal with a chemical shift at 48.10 ppm at pH 6.8, it is separated from the other signals in the spectra from fermentation, and it remains in solution. An appropriate signal size of MeOH relative to other signal sizes was found at $c(\mathrm{MeOH}) = 22.24$ mM. For consistency a modified 0.1 M PBS buffer containing this $c(\mathrm{MeOH})$ (in the following denoted MPBS) was therefore used in all NMR experiments. This is paramount for the quantification process. The 0.1 M PBS is necessary to maintain a physiologically relevant osmolarity and to control pH in the extracellular environment. Large fluctuations in pH renders the chemical surroundings undefined, possibly obscuring identification. Importantly, we tested that MeOH did not interfere with the reactions of fermentation. First, the added amount of MeOH did not alter glycolytic oscillations. Second, using dioxane as a second internal standard, we tested that the ratio of MeOH and dioxane integrals did not change significantly during a fermentation (see section S2 in the SI).

2.7. Quantification

First, integration of a signal (here ^{13}C-lacto) was done by fitting a Lorentzian function to the signal: $f(\delta) = \frac{h\gamma^2}{(\delta-\delta_0)^2+\gamma^2}$, where δ_0 is the center of the signal, h is the height of the signal, and γ is a scale parameter specifying the half-width at half-maximum. This reduced the influence of noise. The integral of the fitted Lorentzian was used as the area of the signal. The area of signal was then related to the area of MeOH by calculating the ratio: $R = \frac{A(\mathrm{signal})}{A(\mathrm{MeOH})}$, where A is the area of the signal. Calculated R-values were used to construct a standard curve and to find concentrations of a species during yeast fermentation.

The standard curve for ^{13}C-lacto was constructed straightforwardly by a series of reactions between 50 mM H^{13}CN and ACA, assuming complete reaction and hence, at equilibration $[\mathrm{ACA}]_0 = [^{13}\text{C-lacto}]$. The ^{13}C-lacto concentration, was plotted against the experimentally determined R. From a linear regression of $[^{13}\text{C-lacto}] = a \cdot R$, the specific a for the particular NMR run-settings was used calculate [^{13}C-lacto] during fermentation.

2.8. Modeling

Building upon previous models of transient glycolytic oscillations [11,8,12], an updated model was manually fitted to capture the new NMR data. The model was simulated on a standard PC using the CVODE solver for stiff ODE systems (SUNDIALS) with a relative tolerance of 10^{-10} and absolute tolerance of 10^{-18}.

2.9. Chemicals

All chemicals were HPLC grade from Sigma-Aldrich (St. Louis, MO, USA), except Glc, glycerol, D_2O, and KCN from Merck (Darmstadt, Germany), fructose-bisphosphate (FBP) and Pyr from Boehringer Mannheim Gmbh (Mannheim, Germany). Finally, ethyl pyruvate is from ICN Biomedicals (Aurora, OH, USA).

3. Results

We used $H^{13}CN$ in both single reaction and fermentation experiments to discriminate between the possible fates of cyanide. Addition of $H^{13}CN$ gave rise to strong signals from cyanide derived species with the chosen recording settings of the ^{13}C-NMR-apparatus. All reactions were carried out in conditions that resembled our fermentation conditions as closely as possible (see Methods). The fermentation process is shown schematically in Fig. 1.

3.1. Chemical shifts of cyanohydrins

From previous studies [13,3,14] as well as our computational models [11,9], it is known that Glc, fructose-6-phosphate (F6P), Pyr, and DHAP are the main carbonyl containing compounds produced during yeast cell fermentation, see Table 1. The ^{13}C-NMR-spectra of these species are shown in Fig. S1. By addition of 5 mM $H^{13}CN$ to 30 mM of these carbonyl containing compounds, the corresponding cyanohydrins were found to have chemical shifts around 117–122 ppm, see Table 2 [15,16], i.e. well separated from the $H^{13}CN$ signal at 111.2 ppm (SI text, section S1.2). As previously found [8], reaction of Glc (or Fru) with cyanide does not readily occur under our conditions. However, small ketones and aldehydes, e.g. DHAP, Pyr, and ACA, react strongly with HCN and the corresponding cyanohydrins of the reaction products have chemical shifts around 120 ppm. Cyanohydrins of sugars have chemical shifts around 118 ppm (Table 2).

3.2. Extracellular signals arising from fermentation of glucose

Fig. 2 shows a ^{13}C-NMR spectrum of the yeast cell suspension before and after fermentation of 25 mM Glc and 5 mM $H^{13}CN$. No ^{13}C-signals are observed before addition of Glc and $H^{13}CN$ and only a single cyanohydrin signal at 120.9 ppm is observed after fermentation. Note that every signal after fermentation could be assigned using spectra of single compounds in 0.1 M MPBS (Fig. S2), although the chemical shifts of signals depended somewhat on the chemical surroundings, i.e. small changes were observed between pure 0.1 M MPBS, yeast cell suspension, and packed yeast cells (see below). The signal from CO_2 at 123.7 ppm, however, was tricky as it is in the range of cyanohydrins. But this signal disappeared if vacuum was applied (Fig. S3) and the approximate range of chemical shift is well-known [17]. Separating supernatant from cells after fermentation shows that a cyanohydrin signal at 120.9 ppm is predominant in the extracellular medium, see Fig. 3A. Occasionally, two tiny additional cyanohydrin signals were also observed. Direct addition of ^{13}C-enriched lacto (produced from reaction between ACA and a small surplus of $H^{13}CN$) increased the area of dominant signal at 120.9 ppm. Nevertheless, it cannot be excluded that signals from other cyanohydrins are masked by the large lacto signal (Δ ppm $\approx$ 0.25 at the base). However, carbonyl containing compounds other than ACA are not known to be excreted directly. In fact, all other carbonyl-containing glycolytic intermediaries are negatively charged,

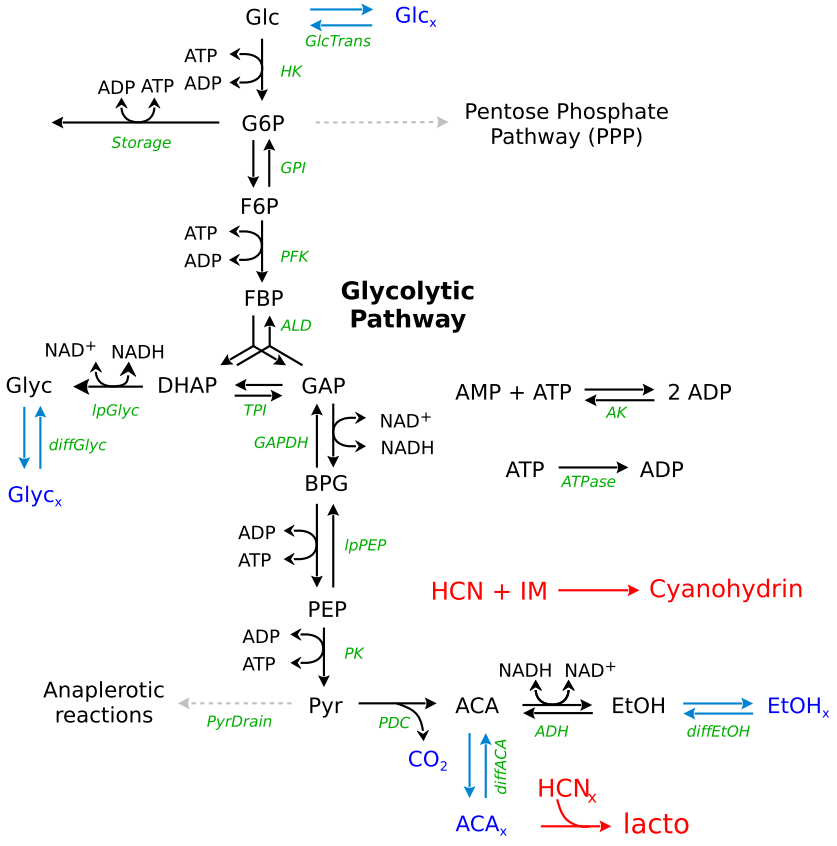

Fig. 1. Schematic of the fermentation process. The reactions shown correspond to the biochemical transformations included in the computational model. Black: glycolytic reactions. Blue: transport reactions and metabolites, Red: cyanide reactions. Intracellular cyanohydrins are unspecified (IM: intracellular metabolite) whereas lacto is the main extracellular cyanohydrin. Enzymatic name abbreviations are shown in green.

Table 1
Intracellular concentration of ketones and aldehydes during fermentation [9]. Ratio between extracellular and intracellular volumes, $\frac{V_e}{V_i} \approx 60$ in our setup.

Metabolite	c_s/mM	Metabolite	c_s/mM
ACA	–	ACA_x	~0.07
Pyr	8.7	DHAP	2.5
F6P	0.5	FBP	5.1

Table 2
Cyanohydrin identification. Chemical shifts of the cyanide carbon of cyanohydrins produced by $H^{13}CN + X \rightleftharpoons {}^{13}CN\text{-}X$ in MPBS.

X	^{13}CN-X [ppm]	X	^{13}CN-X [ppm]
α-D-Glucose	118.4	ACA	120.6
β-D-Glucose	118.8	Pyr	120.9
Fru	None	DHAP	121.0
FBP	119.6	Ribose	118.8

prohibiting passive outflow. This supports previous findings that ACA_x is the major extracellular reactant to cyanide [3,18].

3.3. The extracellular cyanohydrin: quantification of lacto

The stable and well-defined extracellular ^{13}C-lacto signal was not disturbed by the ill-defined $H^{13}CN$ signal [19] (unfortunately, the poor definition of this signal disallowed for simultaneous quantification of $H^{13}CN$). This prompted – with all conceivable reservations – an attempt to estimate the ^{13}C-lacto production by preparation of a standard curve: The literature indicate that the equilibrium constant strongly favors lacto formation (corroborated by our UV-spectroscopy as well) [20,21]. Therefore a standard curve describing the ^{13}C-lacto signal-intensity vs. [^{13}C-lacto] was prepared by reaction of large excesses of $H^{13}CN$ (50 mM) relative to ACA (ensuring virtually complete conversion of ACA to ^{13}C-lacto). The standard curve was found to be linear (Fig. 4A) and was used to estimate extracellular [^{13}C-lacto] during fermentation as seen in Fig. 4B. At the end of the fermentation process, the [^{13}C-lacto] was ~1.5 mM suggesting that most cyanide reacts with ACA_x during fermentation. In [8], however, we reported that about 2 mM to 2.5 mM of free cyanide was removed per 25 mM glucose consumption. Hence, formation of intracellular cyanohydrins equivalent to ~1 mM is estimated.

3.4. Intracellular cyanohydrins

After fermentation of Glc and $H^{13}CN$, at least three intracellular cyanohydrins are observed in ^{13}C-NMR-spectra from packed cells (Fig. 3B). Because the packed cells retain a small fraction of $H^{13}CN$ intracellularly (despite washes), aliquots of either ethyl pyruvate or ACA (both membrane permeable) were then added and allowed to react for 20 min before wash and re-isolation. Fig. 5 shows that ethyl pyruvate addition increases the signal at 120.9 ppm, whereas lacto produced from ACA did not give rise to any increase in intracellular signals. The supernatants also contained a cyanohydrin from reaction with ethyl pyruvate and ACA, respectively. Because a small drift in the DMSO signal, the spectra were aligned such that the chemical shifts of the MeOH signals were 48.1 ppm in every spectrum. DHAP also produce a cyanohydrin at ~121 ppm, but could not be tested as DHAP cannot

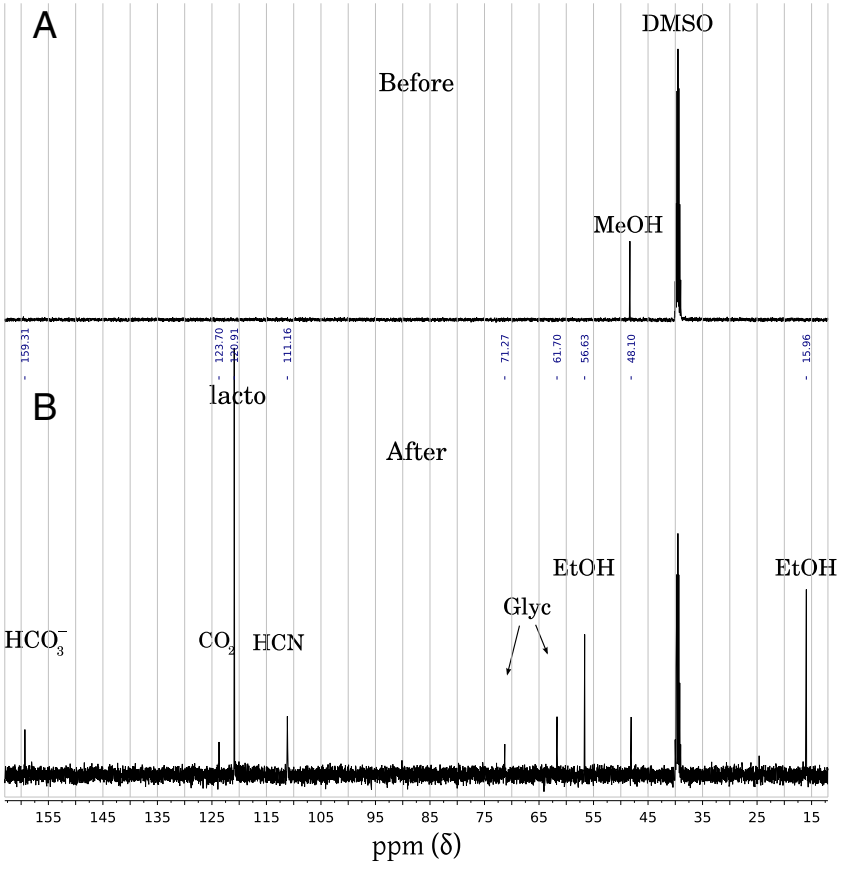

Fig. 2. ^{13}C-NMR spectrum of the yeast suspension before (A) and after (B) fermentation of 24 mM Glc and 5 mM $H^{13}CN$. A: Before fermentation, only the MeOH signal is observed. B: After fermentation, clear signals from the major waste products are observed. Note that only extracellular species are observed.

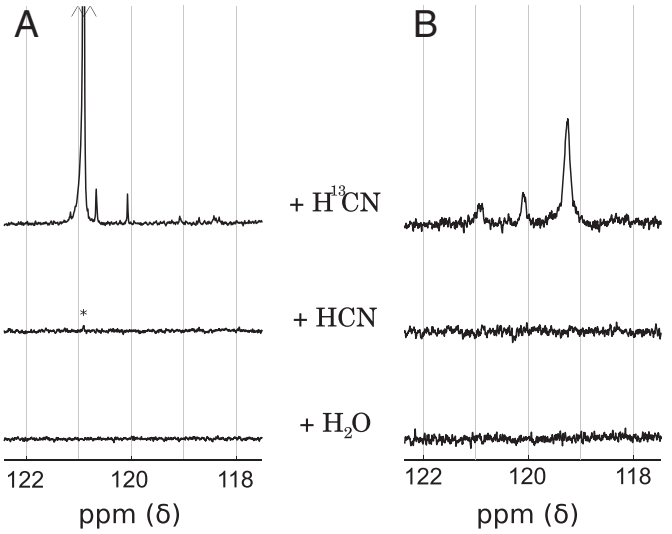

Fig. 3. Extracellular A versus intracellular B cyanohydrins. 45 min after addition of 25 mM Glc and either 5 mM $H^{13}CN$ (upper panel), 5 mM HCN (middle panel) or water (lower panel), the extracellular medium was separated from the yeast cells (subsequently washed twice and resuspended to 500 μl in 0.1 M MPBS) by centrifugation. Both supernatant (A) and packed cells (B) were then subjected to ^{13}C-NMR (NS = 2048 and 4096, respectively). A: Extracellularly, three signals were observed — the largest by far stemming from lacto (120.9 ppm) with the two smaller signals (120.7 and 120.1 ppm) found upfield. With HCN, the lacto signal is only barely visible (*). B: Intracellularly, 3 cyanohydrin signals were observed at 121.0 ppm, 120.1 ppm, and 119.3 ppm.

cross the membrane. However, as [DHAP] is high during fermentation (as opposed to e.g. glyceraldehyde-3-phosphate), it is likely that the peak at 121 ppm in Fig. 5 also contains a DHAP-derived cyanohydrin. The large and relatively broad signal at 119.3 ppm likely derives from cyanohydrins produced by $H^{13}CN$ reacting with various sugars, e.g. ribose, erythrose, FBP etc. (see Table 2).

Unequivocal conclusions about the intracellular cyanohydrin identities are difficult to resolve by straight-forward NMR methods and are outside the scope of this study. Nevertheless, the results are in alignment with the fact that Pyr, DHAP, and various sugars (e.g. phosphates of fructose, gluconolactone, and ribose [22]) are intermediaries found in largest concentrations during fermentation.

3.5. Estimation of [ACA_x] during fermentation

Using spectroscopy, we found that the forward rate constant for the HCN + ACA_x reaction is $k_{f,ACA} \approx 0.11(\text{mM}\cdot\text{min})^{-1}$, and $k_{f,Pyr} \approx 0.035(\text{mM}\cdot\text{min})^{-1}$ for the HCN + Pyr reaction (see example trace in Fig. S5). Thus, lacto production seems to be ~3 times faster compared to PyrCN production (and to our previous estimation using a cyanide electrode [8]). However, due to the inherent inaccuracy of measurement of the reverse rate constant, we were unable to obtain credible differences in K_{eq} for the two reactions. From the measures of the production rate of lacto of ~75 $\frac{\mu M}{min}$, the rate constant of lacto formation ~$0.11(\text{mM}\cdot\text{min})^{-1}$, and [HCN] of ~5 mM, we estimate that [ACA_x] ~ 140 μM during oscillations. Including the reverse rate constant in this equation has no appreciable influence on this estimation of [ACA_x].

3.6. Modeling

Although cyanide is crucial for global oscillations to occur in the stirred suspension of yeast cells, some cells have been observed to show individual oscillations after addition of glucose only [6]. Addition of cyanide, however, increases the proportion of oscillating cells. The present study shows that cyanide binds to carbonyl containing glycolytic metabolites, suggesting a direct effect on the "core" oscillator. We used modeling to address the issue of cyanide mediated synchronization. The following observations were adapted to our average model of yeast cell oscillations (schematic of this model is shown in Fig. 1): a) Fermentation of a 24 mM Glc produces up to 1.5 mM lacto (Fig. 3), whereas total cyanide consumption on average is ~2.5 mM [8]. Thus, intracellular cyanohydrin formation is around 1 mM. b) As no acetate was found extracellularly (Fig. 2), the corresponding reactions were removed. c) During oscillations, the [ACA_x] is on the order of 100 μM. Intracellularly, the lack of quantitative data for cyanohydrin production prompted an unspecific drain of HCN. The impact of increasing the rates of intracellular cyanide reactions with Pyr, DHAP, and ACA on the oscillations was then assessed.

Fig. 6A–D shows dynamic profiles of key metabolites from simulation of the updated average model (see section S4). Note that the amplitude of [ACA_x] oscillations is low despite robust [ACA] and [NADH] oscillations. This becomes important as the average model is expanded into a multicellular model that introduces 5% heterogeneity between the V_{max}'s of individual yeast cells as shown below [12]. Increasing the rate constants of intracellular cyanide reactions with Pyr, DHAP, and ACA while reducing the HCN drain to maintain the same level of overall cyanide consumption, causes a minor but definite increase of the amplitude of NADH oscillations (see Fig. 6E). Due to roughly similar reaction rates between cyanide and Pyr, DHAP and ACA [8] and because [Pyr] > [DHAP] > [ACA] during oscillations, PyrCN is predicted to be the major intracellular cyanohydrin formed as shown in Fig. 6F.

In addition to its role as a bifurcation parameter, addition of cyanide subsequent to glucose could act as a phase resetting event. To test this,

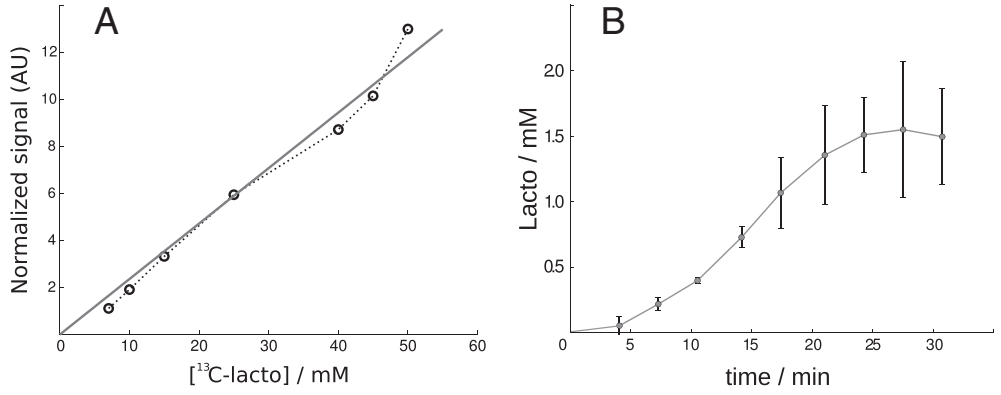

Fig. 4. Fermentation dynamics of extracellular [^{13}C-lacto]. A: A standard curve displaying the normalized signal area $\left(\frac{A(120.9\ \text{ppm})}{A(48.1\ \text{ppm})}\right)$ versus [^{13}C-lacto] showed a linear relationship, allowing for quantitative determination of spectra obtained during fermentation (see Fig. 2). B: Calculated [^{13}C-lacto] profile during fermentation ($n = 3$).

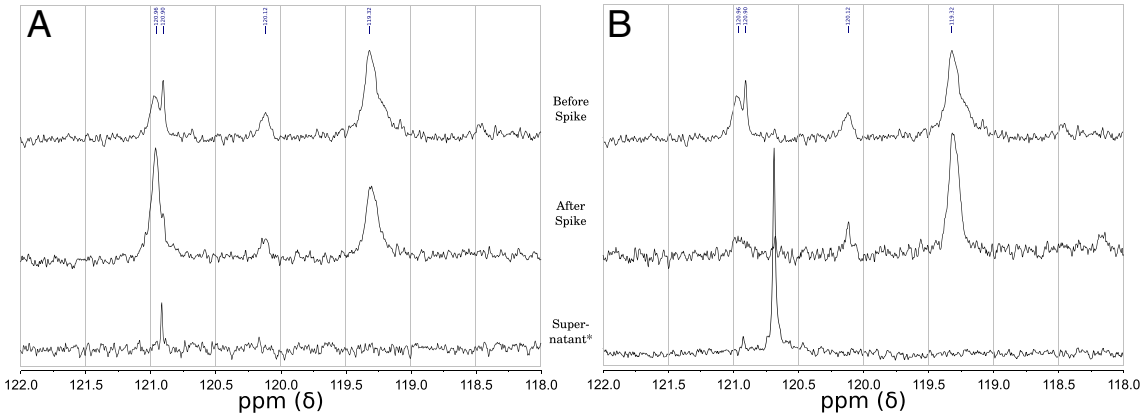

Fig. 5. Identifying intracellular cyanohydrins (all NS = 3560). After a fermentation, the washed yeast cells (as upper panel in Fig. 3B) were subject to extracellular addition of 75 mM ethyl pyruvate (A) or 75 mM ACA (B) and left for >30 min. Cells were then isolated and washed twice in 0.1 M MPBS. Upper panel: Packed cells before external addition (same batch of cells used for both the ethyl pyruvate and ACA addition). Middle panel: Washed, packed cells after the external addition. Lower panel: Supernatant after the external addition. To compare chemical shifts between supernatant and packed cells, the MeOH signal (not shown) was used as a relative reference (volume was increased to 550 μl with 0.1 M MPBS). See text for details.

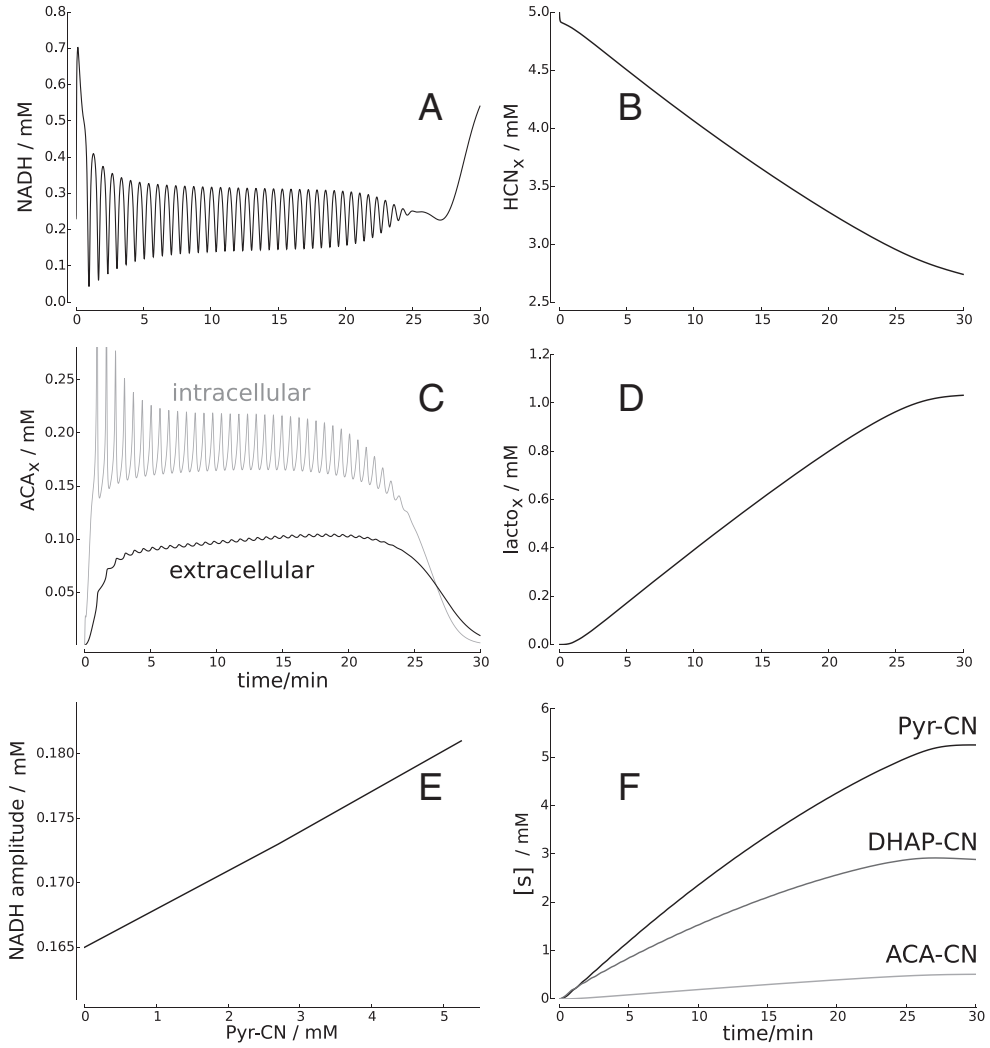

Fig. 6. Simulations of the updated average model. A–D: Simulation-profiles of the transient dynamics of [NADH], [HCN$_x$], [ACA$_x$], and [lacto$_x$], respectively. In C, the black line shows [ACA$_x$] while the gray curve shows intracellular [ACA]. Note that even though robust [NADH] and [ACA] oscillations are present intracellularly, the amplitude of the [ACA$_x$] oscillations is small. E: Intracellular cyanide reactions with Pyr, DHAP, and ACA increase the amplitude of NADH oscillations. A linear relationship between the [NADH] amplitude (measured at $t = 15$ min) and production of intracellular cyanohydrins was found. Here, the amplitude was plotted against [PyrCN], albeit reaction rates of cyanide reactions with Pyr, DHAP, and ACA were all linearly increased. F: PyrCN is predicted to be the major cyanohydrin found intracellularly because [Pyr] is larger than [DHAP] and [ACA] during oscillations.

the average model was expanded into a multicellular model, consisting of 1000 individual and heterogeneous yeast cells, each coupled through ACA_x (the extracellular medium). As shown in Fig. 7A, however, no synchronous NADH oscillations were observed in our simulations (despite a large proportion of individual cells showing pronounced oscillations, see Fig. S7), indicating that either the [ACA_x]-oscillations (Figs. 6C and 7B) are too small to facilitate synchronization between yeast cells or that the sensitivity of the core oscillator to [ACA_x] is too small. Yet, as seen in Fig. 7B, subsequent addition of cyanide produces a sharp decline in [ACA_x] which could act as a global phase-resetting stimulus. This could explain the experimental observation, that cyanide addition subsequent to glucose is a stronger inducer of oscillations compared to cyanide addition simultaneous to (or before) Glc addition (compare Fig. 4A and B in [8]). Yet, in a heterogeneous population of yeast cells, a small amplitude forcing of [ACA_x] oscillations is able to synchronize most cells [12]. This calls for a closer investigation of heterogeneity and the robustness of oscillations in the computational models.

4. Discussion

The emergence of synchronous glycolytic oscillations in a suspension of yeast cells is believed to depend on a reduction in [ACA_x]. While this reduction may be obtained by different means, oscillations are most potently induced by cyanide [6], suggesting additional reactions besides the reaction with ACA_x. Using ^{13}C-NMR, the present study indeed shows that cyanide readily reacts with small sugars and carbonyl containing compounds produced during fermentation (Table 2 and Fig. S2). Such reactions are shown to increase the amplitude of oscillations. Presence of intracellular cyanohydrins was documented after fermentation (Fig. 3). Extracellularly, roughly 2.5 mM cyanide in total is removed during fermentation [8] whereas ~1.5 mM is consumed by [ACA_x]. This shows that synchronized oscillations are dependent on a relatively low [ACA_x], estimated to be >100 μM during oscillations, but also that ~33% of HCN is removed intracellularly. Considering the ease of membrane diffusion, similar rate constants of cyanide reactions to small carbonyl compounds, and the plethora of intracellular electrophile compounds, intracellular removal seems to be somewhat low. Finally, the strong reaction between cyanide and ACA_x suggests that a cyanide addition after glucose can also induce oscillations by acting as a global phase resetting perturbation.

4.1. Extracellular products are visible in ^{13}C-NMR

Fig. 2 shows that extracellular fermentation products display ^{13}C-signals, which were very reproducible between repeated experiments. Remarkably, the chemical shifts of all extracellular signals could be assigned to the known fermentation products (see Fig. S1). Extracellularly, the large signal at 120.9 ppm stems from lacto. Not only is this reaction known to occur extracellularly [3,4,18,5,11,8], direct addition of ^{13}C-enriched lacto also increased the signal area. However, it cannot be excluded that a fraction of the signal arise due to other cyanohydrins having chemical shifts between 120.8 and 121.0 ppm, e.g. from reactions with Pyr or DHAP. As no charged carbonyl containing compounds are known to be released by yeast cells, however, they may also derive from higher alcohols or other substances released in small amounts by fermenting yeast [23]. In principle, the well-defined extracellular signals suggest a use of quantitative 2D HSQR analysis [24,25]. However, the high water content of 0.1 M MPBS severely distorts and hampers ^{1}H-signal detection. Use of D_2O to counter the ^{1}H-signal from H_2O causes yeast cell death. Instead, we employed a simple 1D approach, in which a validated internal reference (here MeOH) is used to construct a standard curve for the compound of interest, in this case ^{13}C-lacto [26]. The use of an internal standard and a validated standard curve for quantitative measures of ^{13}C-NMR-signal may provide a simple and fruitful way of obtaining quantitative data from 1D spectra.

4.2. Dynamics of lacto production using ^{13}C-NMR

The linearity of the ^{13}C-lacto standard curve obtained by reaction of a surplus of H^{13}CN with discrete amounts of ACA (Fig. 4A) allowed for dynamic and quantitative determination of [^{13}C-lacto] during fermentation (Fig. 4B). The slope during fermentation is almost linear (slightly sigmoidal) with a conversion rate of ~75 $\frac{\mu M}{min}$. This compares well with the reported ~60 $\frac{\mu M}{min}$ of lacto production found in the initial phase of fermentation [3] and is also larger than the prediction from our previous models (only 40 $\frac{\mu M}{min}$ from [11] and 5 $\frac{\mu M}{min}$ from [8]). Our experimental findings suggest that [ACA_x] oscillates around 140 μM. However, the assumption that all ACA reacts with H^{13}CN in the production of the ^{13}C-lacto standard curve probably slightly overestimates the lacto measurement (and thus also [ACA_x]). Our model predicts oscillations around 100 μM with an amplitude of 3 μM. This is likely to be too small (intracellularly, the [ACA] amplitude is around 50 μM) which is corroborated by the difficulty of achieving synchronization in our simulations of the multicellular model (Fig. 7) [12]. Previously, a [ACA_x]-range between 50 and 100 μM has been reported [4]. Due to problems with calibration, however, that measurement is uncertain but the range is not far from our [ACA_x] estimate.

4.3. Intracellular cyanohydrin production

Intracellularly, two cyanohydrin signals are observed around ~121 ppm. Fig. 5 strongly suggests that one of them is due to reaction

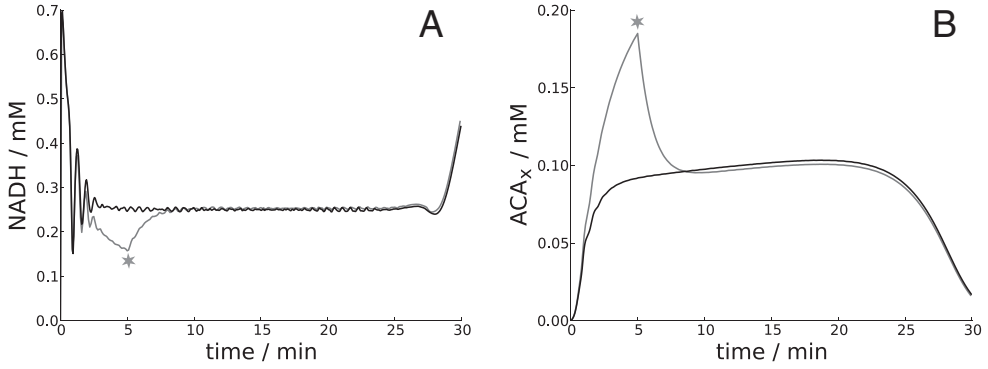

Fig. 7. Simulations of 1000 heterogeneous yeast cells coupled through [ACA_x] in the extracellular medium. A: Average NADH signal from all cells. In the simulations, 5 mM cyanide was either added before 24 mM Glc addition (black line) or 5 min after Glc addition (star, gray line). No oscillations were observed in either case. B: The extracellular [ACA_x] profiles in the two cases of HCN addition.

with Pyr. DHAP also has a relatively high intracellular concentration and produce a cyanohydrin in the same region. The cyanohydrins at 120 ppm and 119.3 ppm are unidentified, but the broad peak of the latter is likely due to reactions with various sugars (see Table 2). Addition of Glc also activates the pentose phosphate pathway, i.e. gives rise to essential sugars such as ribose and erythrose. Thus, a number of sugars could give rise to the broad peak at 119.3 ppm. Notably, lacto was not observed intracellularly, which is surprising as build-up is observed extracellularly (Fig. 2) and during aerobic growth conditions [27]. As opposed to sugars and pyruvate, however, ACA is a highly reactive and volatile compound, suggesting that intracellular [ACA] rapidly drops to zero after fermentation, facilitating a swift destruction of the pH-labile intracellular lacto. Along the same line, the production and extrusion of protons during fermentation stabilize extracellular ACA_x. Indeed, all spectra of intracellular cyanohydrin (Fig. 5) required long-scan times, and thus represent a single snapshot subsequent to the fermentation process and it was not possible to address the intracellular dynamics of cyanohydrin formation.

4.4. Differences in extracellular vs. intracellular cyanohydrin formation

Although we find the lacto formation to be ~3 times faster than PyrCN formation, the rates of cyanide reactions with small glycolytic carbonyl compounds, i.e. ACA and DHAP, are roughly similar [8]. During oscillations, the "effective" concentrations of $[ACA_x]$ and [Pyr] are also similar — in fact, $[Pyr] > [ACA_x] \cdot \frac{V_x}{V_i}$, where V_x,V_i are the extracellular and intracellular volumes, respectively (see Table 1). Therefore, the absence of intracellular cyanohydrin signals in Fig. 2 is somewhat puzzling. The single but large cyanohydrin signal (Fig. 2) resulting from extracellular lacto strongly suggests that intracellular cyanohydrin production mostly serves as minor stores of carbon. Indeed, we previously found that approximately 50% of the 5 mM of added cyanide (i.e. ~2.5 mM) is removed during fermentation of 24 mM Glc [8]. From Fig. 4B, this suggests that approximately 33% and 66% of the added cyanide bind to intracellular species and ACA_x, respectively. Obviously the compartmental division enforced by the plasma membrane provides half of the answer to this discrepancy, but the question of why no more cyanide binds to the plethora of intracellular electrophiles remains. A straight-forward answer is that HCN does not pass the membrane easily, providing for lower intracellular [HCN]. This, however, is unlikely because a) HCN is small molecule with similar polarity to ACA (dipole moments: 2.98 D vs. 2.7 D, respectively) and b) addition of cyanide during quenching experiments is associated with a fast NADH response [11] showing that diffusion across the membrane is fast. A number of causes may be put forth:

a) The diffusion constant of HCN across the plasma membrane is small.
b) The effective rate constants in the cytosol are lower than measured in 0.1 M PBS (or cytosol-like buffer [8]).
c) As HCN is an un-discriminatory nucleophile, the effective intracellular [HCN] is small due to the multiplicity of electrophile substrates.
d) Fermentation enzymes are orchestrated in a complex (as has recently been suggested [28]) that distort normal diffusion processes, i.e. intracellularly the effective [HCN] is small around glycolytic intermediaries.
e) Breakdown of intracellular cyanohydrins. Either by active enzymatic processes or by spontaneous decomposition.

The inability to measure unstable intracellular metabolites quantitatively and the relatively high standard deviation of measurements of extracellular cyanide and lacto necessitates further research to precisely delineate the reaction fates of cyanide during fermentation. Yet, the results confirm intracellular cyanohydrin formation, fitting with high concentration measurements of carbonyl containing glycolytic metabolites (e.g. [Pyr] and [FBP] > 5 mM) during glycolytic oscillations [2,14].

4.5. Cyanide and oscillations

An updated model of transient glycolytic oscillations that largely reproduces the NMR data obtained on extracellular species and lacto formation was developed. It is clear that cyanide lowers $[ACA_x]$ (Fig. 7B) thereby increasing the ratio between the oscillatory amplitude and the average $[ACA_x]$. As NAD^+/NADH is a conserved moiety, a well-balanced level of $[ACA_x]$ is important to drive strong NADH oscillations in the reaction catalyzed by ADH (too much ACA causes high ADH activity and depresses [NADH] and vice versa). Global oscillations require synchronization of phases (and frequencies) of intracellular [ACA] oscillations of individual cells through diffusion of ACA_x. Reducing $[ACA_x]$ is therefore likely to be the key function of agents that induce glycolytic oscillations (additionally, cyanide is likely to provide a more stable removal of ACA_x compared to e.g. bubbling with inert gasses). Another mode of function of cyanide is to react with intracellular carbonyl containing metabolites. We used the updated model to show that intracellular cyanide reactions with Pyr, DHAP, and ACA do enhance the "core" oscillator (Fig. 6E), i.e. increase the amplitude of oscillations.

As was noted in our previous study, cyanide addition after glucose acts as a phase resetting agent due to the simultaneous removal of ACA_x (Fig. 7B), enhancing synchronous, global NADH oscillations [8]. In the multicellular model, however, the coupling strength is too low to allow for entrainment. Even with less heterogeneity introduced between individual cells, the cells drift apart over time. However, the model reproduces the findings that cyanide addition increases the overall NADH signal (Fig. 7A) [11]. Apart from the problem of achieving strong $[ACA_x]$ oscillations in the model or increasing the feedback on the oscillator, two additional problems regarding synchronicity arise: a) is our all-to-all coupling of cells a true representation of reality (stirred cells still have nearest neighbors and most cells are far apart). b) To what extent are yeast cells actually heterogeneous? Regarding the former question, it could be speculated that entrainment of local cells and recruitment of more cells/cell clusters drive the synchronization process, explaining the slow emergence of global oscillations without phase-resetting perturbations. In the latter case, we have no real information of what ways the cells are actually heterogeneous. For example, the relative ease of synchronicity suggests that the frequencies of oscillations are relatively similar is low among yeast cells. This, in turn, suggests that protein expression and enzyme activity is correlated. Development of more comprehensive computational models provide useful tools for analysis of such possibilities. This, however, also requires development of advanced algorithms for optimization of models of transient phenomena.

4.6. Limitations

^{13}C-NMR has low sensitivity compared to ^{1}H or ^{31}P-NMR due to only 1.1% natural abundance of this ^{13}C-isotope, a lower magnetogyric ratio, and its relatively long relaxation times. Moreover, signal intensity distortions usually prohibit quantification. However, the development of the ^{13}C-sensitive CryoProbe™, significantly improves signal-to-noise ratio. Applying identical running conditions and using a carefully chosen internal standard (validated in the relevant concentration ranges) allowed us to compare and quantify the lacto signals from spectra obtained during fermentation. Use of validated internal standards to quantify species has been performed previously in chemical systems [26]. We found accuracy to be very good, while the precision of measurement is more challenging. This is fundamentally related to the signal-to-noise levels of a given spectrum and the quantification process, where precision of fits depends on well-defined signals well above noise. Thus, precision depends on both equipments, the phase-correction procedure, and the system of interest.

5. Conclusions

Using ^{13}C-NMR, we have confirmed that ACA_x is the major source of cyanide removal accounting for ~66% with a conversion rate of ~75 $\frac{\mu M}{min}$. From the kinetics of lacto formation, this corresponds to an $[ACA_x] \approx 140\ \mu M$. Subsequent to fermentation, however, ^{13}C-NMR-spectra of washed and packed yeast cells also showed signals from at least 3 intracellular cyanohydrins. Cyanohydrins formed by reactions of cyanide with Pyr and various sugars (particularly pentoses) are likely candidates for these signals. Although the reduction of $[ACA_x]$ is crucial for inducing global oscillations, these intracellular cyanohydrin reactions are shown to increase the amplitude of NADH oscillations. Lastly, the strong reaction between cyanide and ACA_x suggests that cyanide also may act as a global phase resetting stimulus.

^{13}C-NMR seems to be a promising route for non-invasive measures of dynamical concentration changes in excreted metabolites (of sufficient quantity). Inclusion of such information in comprehensive models remains an important objective in the elucidation of the complex regulation of biochemical pathways and synchronous oscillations.

Supporting information

This paper contains supporting information.

Author contributions

BOH designed the research; AGN and BOH performed the research and analyzed data; BOH, CT and PGS contributed analytic tools; and BOH and PGS wrote the paper.

Acknowledgements

BOH is supported by the Danish Council for Independent Research, Sapere Aude program (DFF-1333-00172 and DFF – 1331-00731B). PGS is supported by the Danish Agency for Science, Technology and Innovation Grant no. 272-07-0487. The authors thank Dorthe Boelskifte for technical assistance. The authors confirm that there are no conflicts of interest.

References

[1] B. Chance, R.W. Estabrook, A. Ghosh, Proc. Natl. Acad. Sci. U. S. A. 51 (1964) 1244–1251.
[2] S. Danø, P.G. Sørensen, F. Hynne, Nature 402 (1999) 320–322.
[3] P. Richard, J.A. Diderich, B.M. Bakker, B. Teusink, K. van Dam, H.V. Westerhoff, FEBS Lett. 341 (1994) 223–226.
[4] P. Richard, B.M. Bakker, B. Teusink, K. Van Dam, H.V. Westerhoff, Eur. J. Biochem. 235 (1996) 238–241.
[5] S. Danø, M.F. Madsen, P.G. Sørensen, Proc. Natl. Acad. Sci. U. S. A. 104 (2007) 12732–12736.
[6] A.-K. Gustavsson, D.D. van Niekerk, C.B. Adiels, F.B. du Preez, M. Goksr, J.L. Snoep, FEBS J. 279 (2012) 2837–2847.
[7] A.K. Poulsen, F.R. Lauritsen, L.F. Olsen, FEMS Microbiol. Lett. 236 (2004) 261–266.
[8] B.O. Hald, M. Smrcinova, P.G. Sørensen, FEBS J. 279 (2012) 4410–4420.
[9] F. Hynne, S. Danø, P.G. Sørensen, Biophys. Chem. 94 (2001) 121–163.
[10] P. Richard, B. Teusink, H.V. Westerhoff, K. van Dam, FEBS Lett. 318 (1993) 80–82.
[11] B.O. Hald, P.G. Sørensen, Biophys. J. 99 (2010) 3191–3199.
[12] B.O. Hald, M.G. Hendriksen, P.G. Sørensen, Bioinformatics 29 (2013) 1292–1298.
[13] M.A. Aon, S. Cortassa, H.V. Westerhoff, J.A. Berden, E.V. Spronsen, K.V. Dam, J. Cell Sci. 99 (Pt 2) (1991) 325–334.
[14] P. Richard, B. Teusink, M.B. Hemker, K.V. Dam, H.V. Westerhoff, Yeast 12 (1996) 731–740.
[15] A.S. Serianni, E.L. Clark, R. Barker, Carbohydr. Res. 72 (1979) 79–91.
[16] A.S. Serianni, H.A. Nunez, R. Barker, J. Org. Chem. 45 (1980) 3329–3341.
[17] M.H. O'leary, R.J. Jaworski, F.C. Hartman, PNAS 76 (1979) 673–675.
[18] S. Danø, F. Hynne, S. De Monte, F. d'Ovidio, P.G. Sørensen, H. Westerhoff, Faraday Discuss. 120 (2001) 261–266.
[19] I. Banyai, J. Blixt, J. Glaser, I. Tth, Acta Chem. Scand. 46 (1992) 142–146.
[20] W.F. Yates, R.L.J. Heider, Am. Chem. Soc. 74 (16) (1952) 41534155.
[21] G. Schlesinger, S.L.J. Miller, Am. Chem. Soc. 95 (1973) 3729–3735.
[22] S. Vaseghi, A. Baumeister, M. Rizzi, M. Reuss, Metab. Eng. 1 (1999) 128–140.
[23] G.M. Walker, Yeast Physiology and Biotechnology, John Wiley & Sons Ltd., 1998
[24] K. Hu, W.M. Westler, J.L. Markley, J. Am. Chem. Soc. 133 (2011) 1662–1665.
[25] I.A. Lewis, S.C. Schommer, B. Hodis, K.A. Robb, M. Tonelli, W.M. Westler, M.R. Sussman, J.L. Markley, Anal. Chem. 79 (2007) 9385–9390.
[26] M.H. Vilhelmsen, J. Jensen, C.G. Tortzen, M.B. Nielsen, Eur. J. Org. Chem. (2013) 701–711.
[27] A. Aranda, M. del Olmo, Appl. Environ. Microbiol. 70 (2004) 1913–1922.
[28] D. Araiza-Olivera, J.G. Sampedro, A. Mjica, A. Pea, S. Uribe-Carvajal, FEMS Yeast Res. 10 (2010) 282–289.